

# Improvement in the manufacture of wax-based fuel for hybrid rockets

Ichiro Nakagawa<sup>\*†</sup> and Yutaro Usui<sup>\*\*</sup>

<sup>\*</sup>Department of Aeronautics & Astronautics, School of Engineering, Tokai University, 4-1-1 Kitakaname, Hiratsuka-shi, Kanagawa, 259-1292 JAPAN

Phone: +81-463-58-1211

<sup>†</sup>Corresponding author: i-nakagawa@tsc.u-tokai.ac.jp

<sup>\*\*</sup>SUZUKI MOTOR CORPORATION, 300 Takatsuka-cho, Minami-ku, Hamamatsu-shi, Shizuoka, 432-8611 JAPAN

Received: February 15, 2017 Accepted: October 2, 2017

## Abstract

Although wax-based fuels for use in hybrid rockets have the desirable property of high regression rate, they are composed of brittle thermoplastic materials that can crack easily in the molding process. Correspondingly, improved manufacturing methods are necessary. In this study, we conducted non-steady thermal conductivity cooling calculations to model the molding process and calculate the maximum thermal stress of such fuels. Our results show that maintaining a higher ambient temperature during the molding process can be effective in reducing cracking. We then conducted tensile testing of microcrystalline wax-based fuel, which has a higher tensile strength than that of normal alkane wax. By adding ethylene vinyl acetate copolymer (EVA) to microcrystalline wax based fuel, we could effectively improve its physical properties. The results of thermal stress analysis using tensile test data showed that it is possible to manufacture a 20% EVA content microcrystalline wax-based fuel with a radius of over 250 mm.

**Keywords:** molding, microcrystalline wax, hybrid rocket

## 1. Introduction

A hybrid rocket has solid fuel and liquid oxidizer. As no explosive materials such as plastics or rubber are used for the solid fuel, hybrid rockets are generally safer than standard rockets. However, hybrid rockets have not found much practical use owing to their inadequate performance as a result of the low regression rate of the solid fuel (that is, the fuel flow rate does not increase sufficiently with oxidizer flow rate). However, the use of wax as hybrid rocket fuel has gained prominent attention since Karabeyoglu et al.<sup>1)</sup> showed that the regression rate of wax is three to four times higher than that of conventional fuels.

Wax, however, is a brittle thermoplastic material in which cracking can easily occur in the molding process owing to high thermal shrinkage. Desain et al.<sup>2)</sup> conducted tensile tests of paraffin wax doped with small concentrations of low density polyethylene (LDPE). The study found that the tensile strength, and elastic modulus increased with increasing concentration of LDPE.

However, the paraffin wax is found to be less elastic than HTPB rubber with a much lower percent elongation.

To improve the relevant physical properties, Maruyama et al.<sup>3)</sup> assessed the application of an admixture of ethylene vinyl acetate copolymer (EVA) to wax. The wax used was a synthesis wax, FT-0070, manufactured by Nippon Seiro Co., Ltd. As it is composed of nearly normal alkane, its properties are similar to those of paraffin wax. The study found that the tensile strength and maximum strain increase as the percentage of EVA content increases, with the former increasing by a factor of about 1.6 and the latter increasing by a factor of up to 2.2 compared with the respective pure wax characteristics when the percentage of EVA content is 20%.

Kim et al.<sup>4)</sup> performed tensile and compression testing with a different type of wax fuel, paraffin-polyethylene blends fuel. They found that both tensile and compressive strength increase with the polyethylene (PE) weight percentage in the fuel, with the corresponding tensile and compressive strengths of 10% PE fuel increased by 42.4

and 42.2%, respectively, compared to the pure paraffin values.

In an effort to eliminate critical size flaws and defects, the manufacturing process of wax grains was studied by Saccone *et al.*<sup>5)</sup> who found that exerting a pressure of about 10 bar during cooling process is effective in addressing such problems.

However, no work to date has focused on the crack-formation mechanism in terms of the relation between thermal stress and tensile strength. In this study, we began from the premise that the tensile strength needs to be larger than the thermal stress occurring during the cooling process of molding in order to prevent the formation of cracks. The thermal stress was estimated through calculations based on the non-steady thermal conductivity cooling model. To obtain tensile strength data, tensile tests were conducted using microcrystalline waxes of varying EVA content. Based on our results, we estimated the cooling temperature of the molding process and the EVA content needed to manufacture fuel grain without cracks.

## 2. Manufacturing process

A spin casting method is generally used to manufacture wax fuel grain. In this study, we employed a method in which microcrystalline wax and EVA are melted and mixed and the mixed liquid is poured into an aluminum circular case that is then set into a spin casting machine and rotated in a constant temperature bath. The melted fuel is solidified pressing against the inner wall of the circular case by centrifugal force. Air bubbles trapped in the melted fuel are then squeezed out, forming a central port. These characteristics of the spin casting process make it a superior method for manufacturing wax-based fuel grain.

After molding, cracks sometimes occur on the inner side of the center port, as shown in Figure 1. To prevent the generation of such cracks, it is necessary to use trial-and-error to select the temperature at pouring, the ambient

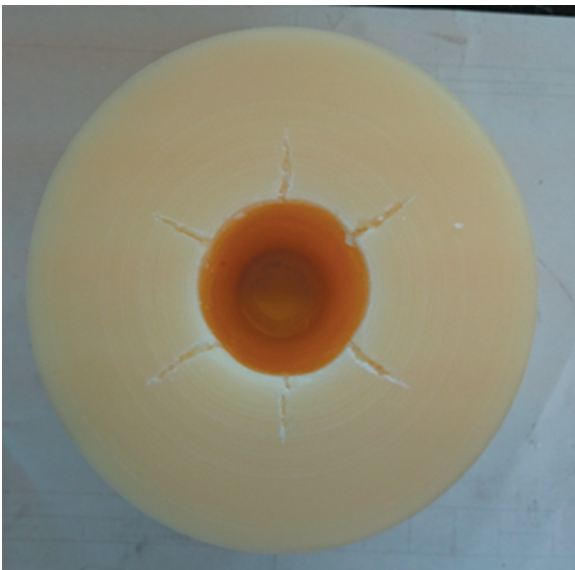


**Figure 1** Cracks which occurred on the inner side of the center port after molding.

temperature during cooling, and the preheating temperature of the case used for molding. However, this takes a long time and creates significant waste material. In particular, it is important to understand the crack-generating mechanism in order to minimize cost and waste of time in manufacturing fuels for use in space transportation that are much larger than those for use in a laboratory.

## 3. Non-steady thermal conductivity cooling calculation

### 3.1 Calculation method

We conducted non-steady thermal conductivity cooling calculations in order to understand the cooling process. We started off by devising a model of the spin casting cooling process in which the liquefied fuel is solidified from the inside and outside surfaces, as shown in Figure 2.

Here, the inner and outer radii are  $r_1$  and  $r_4$ , respectively, and the boundary radial positions between the solid and liquid phases are  $r_2$  and  $r_3$ , respectively.

We divided the fuel cross-section into 40 rings of equal radial width,  $\delta$ . The thermal balance of an individual ring is then given using the following equation :

$$\begin{aligned} \pi (r_{j+1} + r_j) \cdot \lambda \frac{Tr_{j+1} - Tr_j}{\delta} - \pi (r_j + r_{j-1}) \cdot \lambda \frac{Tr_j - Tr_{j-1}}{\delta} \\ = \rho \cdot 2\pi r_j \cdot \delta \cdot c_p \left( \frac{dT}{dt} \right)_{r_j} \end{aligned} \quad (1)$$

where  $r_j$  is the radial position,  $Tr_j$  is the temperature at  $r_j$ ,  $\lambda$  is the thermal conductivity,  $\rho$  is the density, and  $c_p$  is the

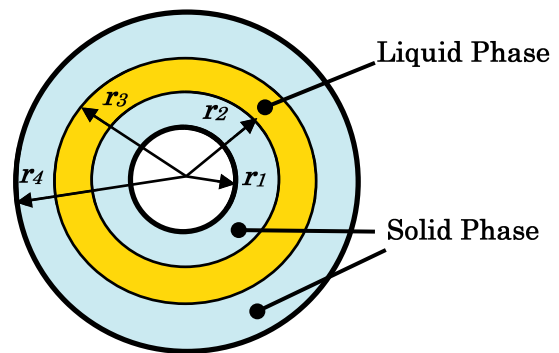


**Figure 2** Model of solidifying process of wax-based fuel.

**Table 1** Material properties of the wax fuel used in the calculation.

(typical values from Nippon Seiro co., ltd. data and Ref. 6)

Properties	Unit	Value
Density-liquid phase	kg m <sup>-3</sup>	800
Density-solid phase	kg m <sup>-3</sup>	900
Melting temperature	K	373
Heat of fusion	kJ kg <sup>-1</sup>	167.2
Specific heat-liquid phase	J kg <sup>-1</sup> K <sup>-1</sup>	2920
Specific heat-solid phase	J kg <sup>-1</sup> K <sup>-1</sup>	2030
Thermal conductivity	W m <sup>-1</sup> K <sup>-1</sup>	0.15
- liquid phase		
Thermal conductivity	W m <sup>-1</sup> K <sup>-1</sup>	0.25
- solid phase		

specific heat. We calculated the temperature of the fuel cross-section using Equation 1 and the following Table 1 data, which are typical values for wax, although not for the specific wax used here.

We solved Equation (1) according to the following initial and boundary conditions:  $T_o$  is the initial temperature of the molding;  $T_1$  is the temperature at the inside;  $T_4$  is the temperature at the outside;  $T_2$  and  $T_3$  are the temperatures at the boundaries between the solid and liquid phases, respectively. We assumed that  $T_o$  is 423 K,  $T_1 = T_4 = T_a$  is the ambient temperature, and  $T_2 = T_3 = 373$  K is the melting point temperature. 423 K is high enough to melt typical wax therefore we heat solid wax up to 423 K usually before casting. The time step was 1 s, and during solidifying, heat which gets into each ring uses to solidify only, therefore  $T_j$  keeps the melting point temperature 373 K.

### 3.2 Calculation results and discussions

The variation in the temperature distribution of the fuel cross-section is shown in Figure 3. Here,  $r_1$  is 20 mm,  $r_4$  is 60 mm, which are our manufacture sample fuel size shown as Figure 1 and  $T_a$  is 313 K which is our typical cooling temperature in casting process. The boundary temperature between the liquid and solid phases is 373 K. The liquid phase nearly disappears at 5,000 s. Figure 4 shows the solid layer thickness vs. time. The outside solid layer is thicker than the inside layer, and solidification is complete at 5,737 s.

The thermal stress is calculated from the following equations<sup>7)</sup>.

$T_2 > T_1$ —the inside solid phase case :

$$(\sigma_t)_{\max} = (\sigma_t)_{r_1} = \frac{\alpha E}{2(1-\nu)} (T_2 - T_1) \beta_1 \quad (2)$$

$$\beta_1 = \frac{2r_2^2}{r_2^2 - r_1^2} - \frac{1}{\ln r_2/r_1}$$

$T_3 > T_4$ —the outside solid phase case :

$$(\sigma_t)_{\max} = (\sigma_t)_{r_4} = \frac{\alpha E}{2(1-\nu)} (T_3 - T_4) \beta_2 \quad (3)$$

$$\beta_2 = \frac{1}{\ln r_4/r_3} - \frac{2r_4^2}{r_4^2 - r_3^2}$$

where  $\alpha$  is the coefficient of linear expansion,  $E$  is the Young's modulus, and  $\nu$  is Poisson's ratio. Here  $\alpha = 4.633E-4$ ,  $E = 165.1$  MPa, and  $\nu = 0.3$  are used by way of example, where the values of  $\alpha$  and  $E$  are measured values for one microcrystalline wax Hi-Mic-2095, which is mentioned later.

The thermal stress vs. time relation is shown in Figure 5, from which it is seen that thermal stress increases with time, reaching a maximum when the liquid layer disappears. The inside thermal stress is always larger than the outside stress, which corresponds to the fact that cracks always occur inside, as shown in Figure 1.

Next, we conducted a non-steady thermal conductivity cooling calculation by changing  $T_a$ . A maximum thermal

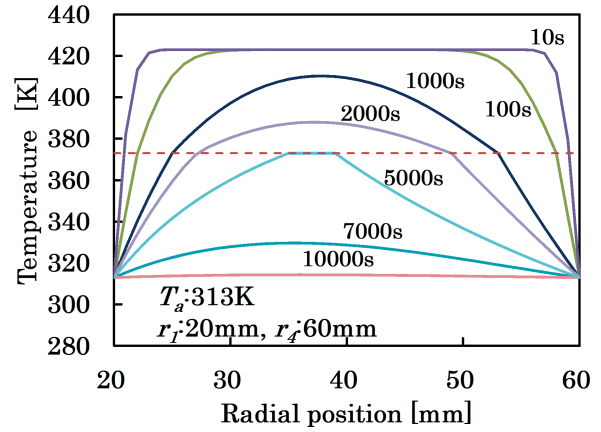


Figure 3 The variation of the temperature distribution.

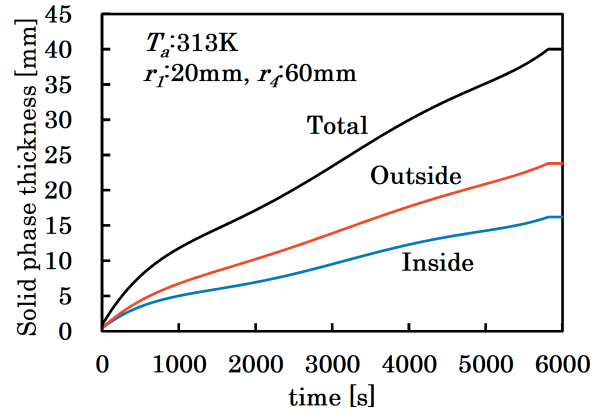


Figure 4 The solid layer thickness vs. time.

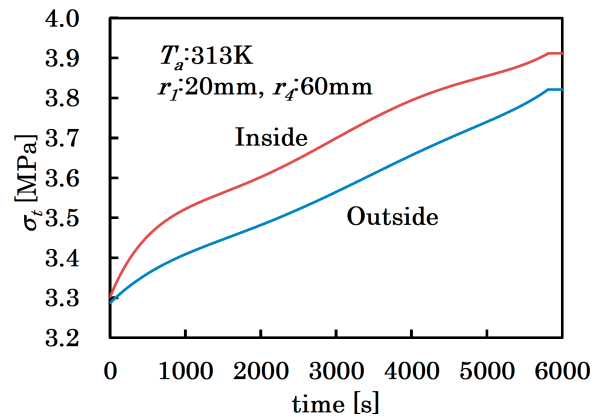
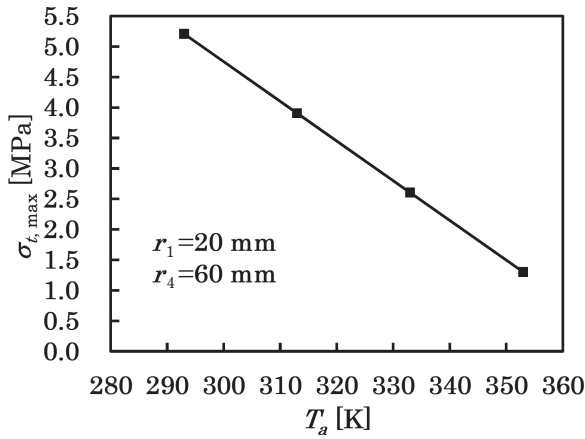


Figure 5 Thermal stress vs. time.

stress analysis was then conducted using the calculated temperature distribution vs. time results. The relationship between the maximum thermal stress and the ambient temperature,  $T_a$ , is shown in Figure 6, from which it is seen that the maximum stress decreases as  $T_a$  rises. The maximum thermal stress at  $T_a = 333$  K is approximately 50% that at  $T_a = 293$  K, or room temperature. Thus, maintaining a higher  $T_a$  that is below the melting temperature during the molding process can be effective in reducing cracking.

### 4. Tensile strength of wax-based fuel

Thermal stress occurs during the wax fuel molding process as calculated above. However, if the tensile strength is larger than the thermal stress, it can be assumed that cracking will not occur.



**Figure 6** The relationship between the maximum thermal stress and  $T_a$ .

Paraffin wax is very common type of wax made from the distillation process of petroleum. Another type of petroleum wax is microcrystalline wax, which is made from residual substances through distillation process. Whereas paraffin wax is primarily composed of normal alkanes, microcrystalline wax is almost completely composed of iso-alkane and cyclo-alkane.

In this study, we conducted tensile tests to evaluate the tensile strength of pure and EVA-mixed microcrystalline waxes in order to estimate the effect on tensile strength of adding EVA to microcrystalline wax.

#### 4.1 Tensile test method

Hi-Mic-2095, made by Nippon Seiro Co., Ltd, was selected as the microcrystalline wax to be used in our tests. It is an inexpensive mass-production material. The main properties of Hi-Mic-2095 are shown in Table 2. As its melting point is the highest among the microcrystalline waxes made by Nippon Seiro Co., Ltd, it is therefore advantageous for use outside on a hot summer day to prevent melting.

EV210ETR, made by Du Pont-Mitsui Polychemicals Co., Ltd, was selected as the EVA. This is a type of EVA that has a high compatibility with wax. As mentioned above, it was used successfully in improving the physical properties of primarily normal FT-0070 alkane wax<sup>3</sup>. EV210ETR is also an inexpensive mass-production material. The main properties of EV210ETR are shown in Table 2.

Tensile tests were conducted in accordance with the "PT-007 simple axis tensile test" standard of the Japan Explosives Society<sup>8</sup>) using a SVZ-50NA tensile and compression tester made by the Imada Factory Co., Ltd. The pulling speed was adjusted to 10 mm s<sup>-1</sup>, which is the lowest speed of the machine.

**Table 2** Main properties of the fuel and the additive.

	Chemical formula	Melting point [K]	Density [kg m <sup>-3</sup> ]
Hi-Mic-2095	C <sub>44</sub> H <sub>90</sub>	374	955
EV210ETR	C <sub>5</sub> H <sub>7</sub> O <sub>2</sub> (CH <sub>3</sub> )	346	950

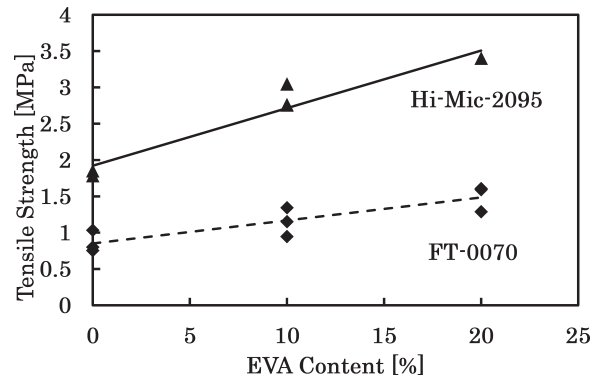


**Figure 7** Relationship between tensile strength and EVA content.

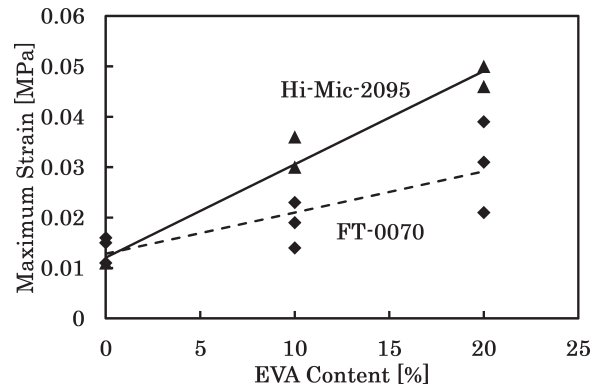


**Figure 8** Relationship between maximum strain and EVA content.

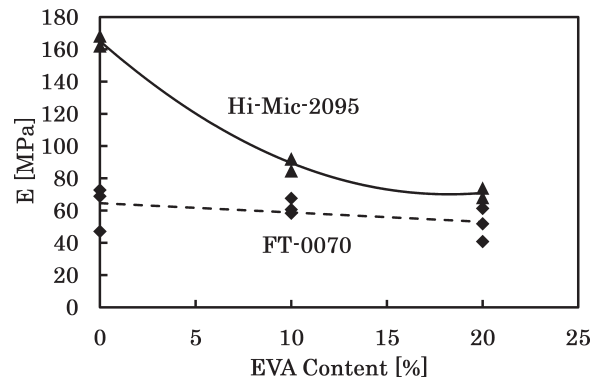


**Figure 9** Relationship between Young's modulus (E) and EVA content.

#### 4.2 Tensile test results

Figure 7 shows a comparison of our tensile strength results with those of the FT-0070 data of Maruyama *et al.*<sup>3</sup>) The tensile strength of pure Hi-Mic-2095 is approximately twice that of pure FT-0070 and increases as the EVA content increases, with the tensile strength of EVA 20% content Hi-Mic-2095 based-fuel a little more than twice that of pure Hi-Mic-2095.

The maximum strain values are shown in Figure 8, from which it is seen that the maximum strain of pure Hi-Mic-2095 is nearly identical to that of pure FT-0070. However, the maximum strain of EVA 20% content Hi-Mic-2095 based-fuel is approximately 1.7 times that of EVA 20% content FT-0070 based-fuel.

Young's modulus (E) is shown in Figure 9. The E of Hi-Mic-2095 based-fuel decreases steeply as EVA content increases up to 10%, after which it decreases slowly up to

an EVA content of 20%. On the other hand, the E of FT-0070 based-fuel decreases only a little as EVA content increases.

### 5. Results and discussion

We suggest that the variation of the temperature distribution during the molding process as a result of adding EVA is small because the EVA-induced changes in thermophysical properties such as  $\lambda$ ,  $c_p$ , and  $\rho$  are small, as both wax and EVA are plastic and composed almost entirely of C and H. In this case, the change in thermal stress as a result of adding EVA to Hi-Mic-2095 can be calculated from Equations (2) and (3), using the above tensile test data and the calculated temperature distribution. The relationship between maximum thermal stress and tensile strength as a result of adding EVA to Hi-Mic-2095 is shown in Figure 10, where  $T_a$  is 293 K,  $r_1$  is 20 mm, and  $r_4$  is 60mm. The maximum thermal stress decreases with added EVA and becomes lower than the tensile strength at an EVA content of approximately 10%. Thus, it can be assumed that cracking does not occur at above 10% EVA content Hi-Mic-2095 based fuel in this case.

The change in maximum thermal stress as a function of  $r_4$  was calculated for  $T_a = 293$  K, in which room temperature tensile tests were conducted and  $r_1 = 20$  mm at  $r_4 = 40, 60, 100, 140,$  and  $180$ mm which are variables based on our manufacture sample fuel size. The maximum thermal stress relation of EVA 10% content fuel is shown in Figure 11, from which it is seen that the maximum

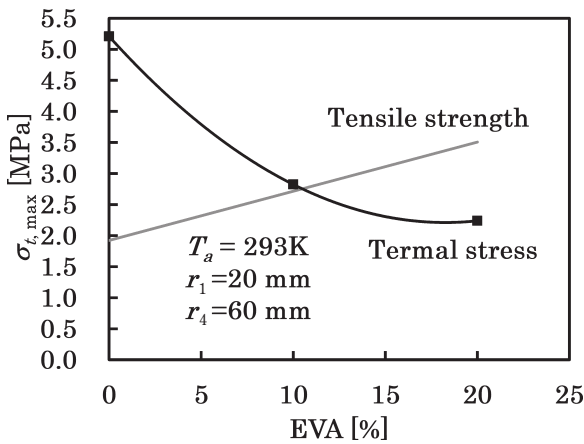


Figure10 Thermal stress and tensile strength vs. EVA content.

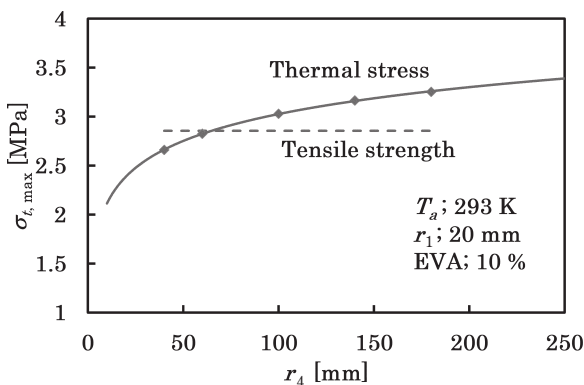


Figure11 Fuel outer diameter effect of EVA 10 % fuel.

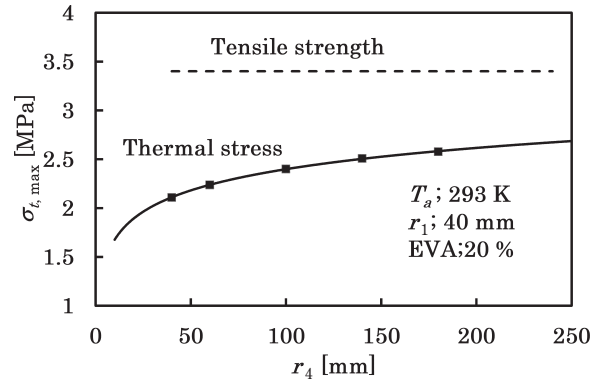


Figure12 Fuel outer diameter effect of EVA 20 % fuel.

thermal stress increases as  $r_4$  increases. The tensile strength is lower than the maximum thermal stress at  $r_4 > 60$  mm, suggesting that cracks can occur in this region. The corresponding relation for EVA 20% content fuel is shown in Figure 12. Here, the tensile strength is higher even at  $r_4 = 250$  mm, suggesting that cracks cannot occur in this region and, therefore, that it is possible to successfully mold fuels of this size which is considered to be minimum size for a space launch rocket, for example SS-520 of JAXA.

### 6. Conclusions

Based on a model of the cooling process of the spin casting method, we conducted non-steady thermal conductivity cooling calculations to determine the maximum thermal stress. Our results showed that the maximum thermal stress decreases as  $T_a$  increases, with the maximum thermal stress at  $T_a = 333$  K approximately 50% of that at  $T_a = 293$  K (room temperature). This suggests that maintaining the higher  $T_a$  below the melting temperature during the molding process can be effective in reducing cracking.

The tensile strength, maximum strain, and Young's modulus (E) of Hi-Mic-2095 based-fuel were obtained through tensile testing. We determined that the tensile strength of pure Hi-Mic-2095 is approximately twice that of pure FT-0070 and increases as the EVA content increases, with the tensile strength of EVA 20% content Hi-Mic-2095 based-fuel reaching a value of slightly greater than twice that of pure Hi-Mic-2095. Although the maximum strain of pure Hi-Mic-2095 is nearly identical to that of pure FT-0070, the maximum strain of EVA 20% content Hi-Mic-2095 based-fuel is approximately 1.7 times that of EVA 20% content FT-0070 based-fuel. The Young's modulus of Hi-Mic-2095 based-fuel decreases steeply as the EVA content increases up to 10% then decreases slowly up to 20%.

Finally, a thermal stress analysis of the variation of  $r_4$  was conducted using tensile test data. The tensile strength of EVA 20% content Hi-Mic-2095 based-fuel is higher than the thermal stress even at  $r_4 = 250$  mm, suggesting that cracks cannot occur in fuels of up to this radius and, therefore, that it is possible to successfully mold fuels of this size.

Overall, our results suggest that maintaining  $T_a$  at

higher than room temperature and adding EVA are both effective in successfully molding wax fuel for use in space transportation that are much larger than those for use in a laboratory.

### Acknowledgment

This research is supported by the Hybrid Rocket Research Working Group (HRrWG) of Institute of Space and Astronautical Science, Japan Aerospace Exploration Agency. The authors thank members of HRrWG for their helpful discussion.

### Reference

- 1) M. A. Karabeyoglu, B. J. Cantwell, and D. Altman, 37th AIAA/ASME/SAE/ASEE Joint Propulsion Conference and Exhibit, AIAA Paper 2001–4503 (2001).
- 2) J. D. DeSain, B. B. Brady, K. M. Metzler, T. J. Curtiss, and T. V. Albright, 45th AIAA/ASME/SAE/ASEE Joint Propulsion Conference and Exhibit, AIAA Paper 2009–5115 (2009).
- 3) S. Maruyama, T. Ishiguro, K. Shinohara, and I. Nakagawa, 47th AIAA/ASME/SAE/ASEE Joint Propulsion Conference and Exhibit, AIAA Paper 2011–5678 (2011).
- 4) S. Kim, H. Moon, J. Kim, and J. Cho, *J. Prop. and Power*, 31, 1750–1760 (2015).
- 5) G. Saccone, F. Piscitelli, A. Gianvito, G. Cosentino, and L. Mazzola, 51th AIAA/ASME/SAE/ASEE Joint Propulsion Conference and Exhibit, AIAA Paper 2015–4039 (2015).
- 6) M. A. Karabeyoglu, D. Altman, and B. J. Cantwell, *J. Prop. and Power*, 18, 610–620 (2002).
- 7) I. Nakahara, “Zairyo Rikigaku Gekan”, 103–104, Yokendo (1968).
- 8) Japan Explosives Society, “Standard of Japan Explosives Society (V)”, 30–33 (1996).